BIOCHEMISTRY
including biophysical chemistry & molecular biology

Article

pubs.acs.org/biochemistry

A Conserved Amphipathic Ligand Binding Region Influences K-Path-Dependent Activity of Cytochrome *c* Oxidase

Carrie Hiser,[†] Leann Buhrow,[†] Jian Liu, Leslie Kuhn, and Shelagh Ferguson-Miller*

Department of Biochemistry and Molecular Biology, Michigan State University, East Lansing, Michigan 48824, United States

Supporting Information

ABSTRACT: A conserved, crystallographically defined bile acid binding site was originally identified in the membrane domain of mammalian and bacterial cytochrome *c* oxidase (C*c*O). Current studies show other amphipathic molecules including detergents, fatty acids, steroids, and porphyrins bind to this site and affect the already 50% inhibited activity of the E101A mutant of *Rhodobacter sphaeroides* C*c*O as well as altering the activity of wild-type and bovine enzymes. Dodecyl maltoside, Triton X100, C12E8, lysophophatidylcholine, and CHOBI-MALT detergents further inhibit *Rs*C*c*O E101A, with lesser inhibition observed in wild-type. The detergent inhibition is overcome in the presence of micromolar concentrations of steroids and porphyrin analogues including deoxycholate, cholesteryl hemisuccinate, bilirubin, and protoporphyrin IX. In addition to alleviating detergent inhibition, amphipathic carboxylates including arachidonic, docosahexanoic, and phytanic acids stimulate the activity of E101A to wild-type levels by providing the missing carboxyl group. Computational modeling of dodecyl maltoside, bilirubin, and protoporphyrin IX into the conserved steroid site shows energetically favorable binding modes for these ligands and suggests that a groove at the interface of subunit I and II, including the entrance to the K-path and helix VIII of subunit I, mediates the observed competitive ligand interactions involving two overlapping sites. Spectral analysis indicates that ligand binding to this region affects C*c*O activity by altering the K-path-dependent electron transfer equilibrium between heme *a* and heme a_3. The high affinity and specificity of a number of compounds for this region, and its conservation and impact on C*c*O activity, support its physiological significance.

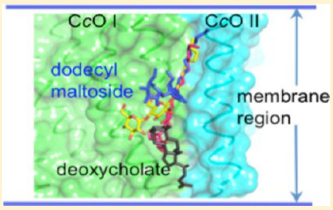

The recent observations of specific conserved lipid binding sites in high-resolution X-ray structures of cytochrome *c* oxidase[1−5] expands our vision of how lipidic ligands may control the activity of membrane proteins[6] and offers an explanation for earlier reports of lipid and detergent effects on C*c*O activity.[7−11]

An interesting finding in this regard is that cholate, a bile acid detergent that is used to purify bovine C*c*O (bovC*c*O) and observed to strongly inhibit the enzyme,[12] is resolved in all crystal structures of the bovine enzyme (e.g., ref 1, PDB: 10CC, 2DYR, 3AG2, and 2Y69). One of the two best-resolved cholate binding sites is close to the entrance of the K-path, a proton uptake pathway that is essential for activity. This cholate molecule forms a tight hydrogen bond with the carboxyl group of E62, homologous to E101 in the *Rhodobacter sphaeroides* C*c*O (*Rs*C*c*O). This conserved residue is found by mutagenesis to be important in K-path function.[13−16] The positioning suggests that the inhibitory effect of cholate observed in bovine C*c*O is due to blockage of the K-path, preventing the proton uptake that is required to support electron transfer from heme *a* to heme a_3.[13,17−19]

When cholate was first noted in the bovC*c*O structure, the idea was put forward that it could represent an adenine nucleotide binding site.[1] Adenine nucleotides had been observed to regulate the activity of the mammalian enzyme,[20−25] although inhibition or regulation of the K-path was not suggested at that time.

Removal of the carboxyl group of E101 in subunit II by mutagenesis inhibits K-path function.[13] Under standard assay conditions, the activity of the E101A mutant of *Rs*C*c*O is 5−8% of wild-type (WT) C*c*O.[14,16] Unexpectedly, it was discovered that micromolar levels of cholate or deoxycholate (DOC) stimulated the activity of this mutant by 10-fold.[16,26] The apparent chemical rescue of the mutant's activity at such low concentrations suggested that these bile acids were binding close to the missing carboxyl group at the right position to serve as the needed proton acceptor/donator in the K-path. Indeed, crystals of *Rs*C*c*O grown in the presence of DOC showed a single DOC molecule bound as expected for chemical rescue, with its carboxyl group located close to that of E101 and in a similar location as cholate in the bovC*c*O.[26] The conservation of a bile acid/steroid binding site in such a key position added weight to the concept that this site may have physiological significance.

To further investigate the nature and significance of this conserved site in C*c*O, we have used the *Rs*C*c*O mutant E101A as a sensitive assay system for compounds that bind in the site, as indicated by activation, inhibition, or competition. In the absence of high-resolution crystal structures of *Rs*C*c*O with other lipidic regulatory molecules besides bile acids in this site, we have characterized the site computationally and determined favorable binding modes for other observed ligands. The results show that a number of amphipathic molecules, lipids, and

Received: October 24, 2012
Revised: January 23, 2013
Published: January 27, 2013

   dx.doi.org/10.1021/bi3014505 | *Biochemistry* 2013, 52, 1385−1396

detergents compete in the micromolar concentration range, causing loss or regain of CcO activity via specific interactions at or near this critical conserved site at the entrance of the K-path.

MATERIALS AND METHODS

Purification of CcO. *Rhodobacter sphaeroides* strains overexpressing the 37-2 WT CcO[27] or the E101A mutant CcO[16] were grown, and cell membranes were prepared as described;[27] the *Rs*CcO was isolated by metal affinity chromatography as described for crystallography.[16] Bovine heart CcO was purified according to Suarez et al.[28]

Activity Assays. Oxygen uptake rates were measured with a Clark-type electrode and turnover rates (TN, electrons per second per CcO molecule) calculated as described.[29] Assay mixtures contained 100 mM HEPES pH 7.4, 24 mM KCl, 2.8 mM ascorbate, 5.6 μM EDTA, 1 mM *N,N,N′,N′*-tetramethyl-*p*-phenylenediamine (TMPD) with 30 μM bovine heart cytochrome *c* as the substrate, and with varying levels of dodecyl maltoside (DDM; 0.06% final concentration was used in the "standard" assay) and other additives as noted. Higher EDTA levels were tested in the assay but did not affect the behavior of WT or mutant CcO with or without added ligands.

The additives used in activity studies include lyso-oleoyl phosphatidylcholine (18:1 lysophosphatidylcholine, lyso-PC) and asolectin from Avanti Polar Lipids (Alabaster, AL), high-purity 10% Triton X100 from ThermoScientific/Pierce (Rockford, IL), arachidonic and docosahexanoic acids from Cayman Chemicals (Ann Arbor, MI), and CHOBIMALT, DDM, decyl maltoside (DM), and Anapoe 20 (Tween 20) from Anatrace/Affymetrix (Maumee, OH). Other additives were from Sigma-Aldrich (St. Louis, MO). The chemicals structures of all additives are listed in Supporting Information Table T1.

Spectral Reduction Assays. The steady-state reduction levels of hemes were compared by using a variation of the method of Konstantinov et al.[17] Assays were performed in 100 mM CHES pH 9.5, with 0.01% DDM, 1 mM ascorbate, and 200 μM TMPD, with and without CHOBIMALT, in an unstirred cuvette in a PerkinElmer Lambda 40 spectrophotometer. Curves were aligned to 462 and 621 nm for the Soret and α peaks, respectively, and then normalized to the fully reduced α peak (607 nm minus 630 nm, indicative of enzyme concentration) so that different enzymes and conditions could be compared.[17]

Protein and Ligand Structures. The crystal structures of bovine CcO (PDB: 2DYR[5]), *Rs*CcO with (PDB: 3DTU[26]) and without (PDB: 2GSM[2]) deoxycholate, and *Paracoccus denitrificans* CcO (PDB: 3HB3[4]) were used for ligand binding and flexibility analysis. Crystal structures of ferrochelatase in complex with cholate (PDB: 2PO7[30]) or heme (PDB: 2QD2[31]) and serum albumin in complex with biliverdin (PDB: 2VUE[32]) or fusidic acid (PDB: 2VUF[32]) were used for ligand docking. Decyl maltoside, dodecyl maltoside, biliverdin, and protoporphyrin IX ligand structures were obtained from the above structures.

***SLIDE* Small Molecule Docking.** The groove between subunits I and II in the crystal structure of *Rs*CcO with bound deoxycholate removed (PDB: 3DTU[26]) was used as the target for *SLIDE* (Screening Ligands by Induced-fit Docking, Efficiency) prediction of the binding modes of experimentally identified ligands.[33,34] *SLIDE* characterizes a binding pocket by a template of chemistry-labeled points that are favorable positions for protein−ligand hydrophobic interactions or hydrogen bonds. In this work, the known interactions of deoxycholate or dodecyl maltoside were used to create the template. To sample ligand flexibility fully, low-energy conformations of all docked ligands were generated using *Omega* (OMEGA version 2.0. OpenEye Scientific Software, Santa Fe, NM[35]). Using distance and geometric constraints, *SLIDE* predicts the orientation of ligand binding by sampling all orientations that yield good shape and chemical complementarity between the ligand and protein and then chooses the orientation of the conformer with the most favorable $\Delta G_{binding}$ according to *SLIDE's* OrientScore [Tonero et al., in preparation]. *SLIDE* AffiScore, a weighted sum of favorable polar and hydrophobic interactions and unfavorable (unsatisfied/repulsive) interactions between the protein and ligand, was used to assess the relative $\Delta G_{binding}$ of these diverse ligands in the binding groove.

Ligand Transposition. To test whether porphyrin-like ligands could mimic the steroid ring interaction in *Rs*CcO, comparisons were made to other proteins in which both these types of ligands have been found to occupy the same site. Serum albumin and ferrochelatase have been crystallized in separate complexes with steroid and heme-like ligands in a single binding site (see Protein and Ligand Structures section). The overlaid ligands were transposed into the *Rs*CcO steroid site, in the same orientation as they exhibit in serum albumin and ferrochelatase. The bound cholate in ferrochelatase (PDB: 2PO7[30]) and bound fusidic acid in serum albumin (PDB: 2VUF[32]) were aligned to the *Rs*CcO deoxycholate (PDB: 3DTU[26]) based on least-squares fitting of their steroid ring atoms using *OEChem RMSD* (RMSD version 1.7.2.4. OpenEye Scientific Software, Santa Fe, NM[35]). Ferrochelatase with bound protoporphyrin IX (PDB: 2QD2[31]) was superimposed onto ferrochelatase with bound cholate, and serum albumin with bound biliverdin (PDB: 2VUE[32]) was superimposed onto serum albumin with bound fusidic acid (PDB: 2VUF[32]), based on least-squares fitting of their protein backbone atoms using *PyMOL* molecular graphics software (Schrödinger, Inc., New York). Whether the heme ligands were sterically permitted and energetically favorable in this orientation was then assessed using *PyMOL* and *SLIDE* prediction of $\Delta G_{binding}$, respectively.

***Consurf* Amino Acid Conservation and *ProFlex* Flexibility Analysis.** The amino acid conservation and flexibility of the CcO main chain were evaluated using the *Consurf* [36] and *ProFlex*[37] methods, respectively, as described in Buhrow et al.[38] Over 250 amino acid sequences of CcO were used for conservation analyses as described in Buhrow et al.[38]

RESULTS

Bile Acid Structural Specificity for Stimulating E101A *Rs*CcO Activity. To elucidate the structural specificity for the observed stimulation of the E101A mutant of *Rs*CcO, activity was measured with a variety of bile acids at 250 μM final concentration under standard assay conditions (Table 1). The effect on E101A activity was highly sensitive to the position and stereochemistry of hydroxyl groups on the steroid ring and to the length of the carboxyl tail (Supporting Information Table T1). Cholate and deoxycholate[26] remained the strongest effectors at this concentration. Only chenoDOC and lithocholate were close to their effectiveness (~10-fold stimulation); taurocholate stimulated only 3-fold, and GUDCA stimulated by 40%. UrsoDOC and glycochenoDOC had no observable effect. The most potent effector, deoxycholate (Figure 1), caused no change in the spectral properties of oxidized or reduced E101A. All the bile acids

dx.doi.org/10.1021/bi3014505 | *Biochemistry* 2013, 52, 1385−1396

Table 1. Effects of Bile Acids on the Activity of the E101A Mutant and WT *Rs*CcO[a]

bile acid additive	*Rs*CcO E101A activity ($e^-/s/aa_3$)	*Rs*CcO WT activity ($e^-/s/aa_3$)
buffer	60 ± 10	1270 ± 20
cholate	800 ± 10	1260 ± 10
deoxycholate (DOC)	780 ± 20	1210 ± 20
chenoDOC	620 ± 60	1240 ± 30
lithocholate[b]	530 ± 60	1150 ± 80
taurocholate	150 ± 10	1360 ± 80
glycoursoDOC (GUDCA)	90 ± 40	1160 ± 40
glycochenoDOC	60 ± 30	1360 ± 60
ursoDOC	50 ± 10	1260 ± 60

[a]Purified *Rs*CcO was assayed in 0.06% DDM as described in Materials and Methods in the absence (buffer) or presence of 250 μM of each bile acid. All numbers are means ± one standard deviation of at least three assays. [b]Due to its poor solubility, lithocholate was added to a final concentration of only 75 μM.

tested had no significant effect on WT *Rs*CcO activity at 250 μM concentration under these conditions. Their differential effect on the mutant presumably was due to their ability to chemically rescue the missing carboxyl group in E101A, involved in proton uptake at the entrance of the K-path where crystal structures show bile acids to bind.

Other Lipidic and Heterocyclic Compounds Affect E101A *Rs*CcO Activity. Other lipidic and heterocyclic compounds with carboxyl functional groups were tested for their ability to differentially stimulate the activity of E101A under the standard assay conditions (Figure 1A). Among those tested, the cholesterol mimic cholesteryl hemisuccinate (CHS) stimulated E101A even more effectively than cholate, to an activity of ~500 s^{-1} with half-maximal stimulation ($K_{1/2}$) at ~80 μM, as compared to 200 μM for cholate. Since some structural and binding similarities between porphyrins and steroids have been observed (ferrochelatase, serum albumin, heme oxygenase[30−32]), the heme precursor protoporphyrin IX (PPIX) was tested. It also stimulated E101A more potently than bile acids ($K_{1/2}$ ~ 14 μM); the heme breakdown product bilirubin (BR) stimulated to a lesser degree (to ~180 s^{-1} with $K_{1/2}$ ~ 50 μM).

Bile acids, PPIX, BR, and CHS had no significant effect on the activity of the D132A mutant of *Rs*CcO (data not shown), even though mutation of that carboxyl group at the entrance of the D proton uptake pathway had been previously shown to be very effectively rescued by arachidonic and docosahexanoic acids but not the corresponding alcohols.[39] Although the steroid/porphyrin-related compounds did not rescue D132A, the long chain unsaturated fatty acids were tested and found to rescue E101A as well as D132A (Figure 1B). Therefore, the steroid binding appears quite specific for the K-path entrance region, while the more flexible long-chain fatty acids show high affinity for the vicinity of both proton entry pathways.

As in the case of the long-chain fatty acids arachidonic and docosahexanoic acids (Figure 1B), the 20-carbon branched-chain isoprene compound phytanic acid, known to modulate pathways of steroid and lipid synthesis,[40−42] was found to be a surprisingly powerful effector of E101A (Figure 1B), stimulating to an activity of >1000 s^{-1} (~20× nonadditive rates) with half-maximal stimulation at ~4 μM. Phytol, a phytanic acid precursor without a carboxyl group, had little effect at the same micromolar concentrations, and as seen with the bile acids, phytanic acid at micromolar levels did not stimulate the D132A mutant (data not shown). Retinoic acid, another isoprene compound and known regulator of lipid and steroid metabolism,[43] also strongly stimulated E101A activity ($K_{1/2}$ ~ 8 μM) (Figure 1B) with little effect on D132A or WT activity (data not shown). The high-affinity ligands shown in panel B stimulated to close to WT activity, indicating strong repair of the carboxyl mutation.

These results (Figure 1A,B), including the differential selectivity of the D- and K-path chemical rescue, indicate a significant difference in the binding site characteristics of the two proton pathway entrance regions. The D-path associated binding site (whose exact location is not known) appears more constricted, only accommodating unbranched functional groups, while the K-path binding site appears substantially larger, accommodating not only long-chain polyunsaturated

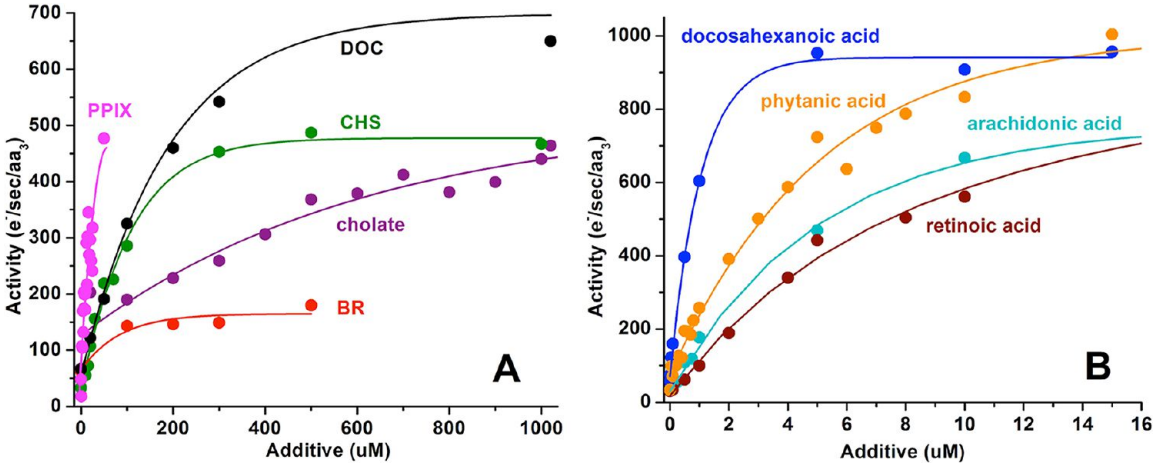

Figure 1. Stimulation of E101A *Rs*CcO by amphipathic carboxylates in 0.06% DDM. Purified E101A *Rs*CcO was assayed in 0.06% DDM as described in Materials and Methods. Panel A: bilirubin (BR; red), cholate (purple), cholesteryl hemisuccinate (CHS; green), deoxycholate (DOC; black), protoporphyrin IX (PPIX; magenta). Panel B: arachidonic acid (cyan), docosahexanoic acid (blue), phytanic acid (orange), retinoic acid (brown). Note different concentration and activity axes in panels A and B; higher affinity ligands are shown in panel B. The starting activities in the absence of ligand ranged from 31 to 66 s^{-1}.

dx.doi.org/10.1021/bi3014505 | *Biochemistry* 2013, 52, 1385−1396

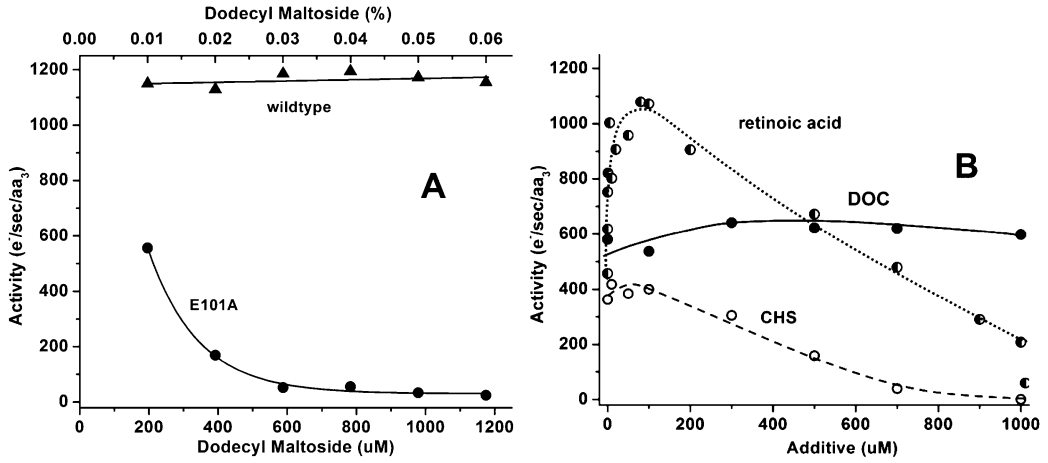

Figure 2. Effects of DDM (A) and amphipathic carboxylates in low DDM (B). Purified E101A (circles) and WT (triangles) *Rs*C*c*O were assayed in 0.01% DDM as described in Materials and Methods. Additive in panel A: DDM; additives in panel B: cholesteryl hemisuccinate (CHS; open circles, dashed line), deoxycholate (DOC; solid circles, solid line), retinoic acid (half-filled circles, dotted line).

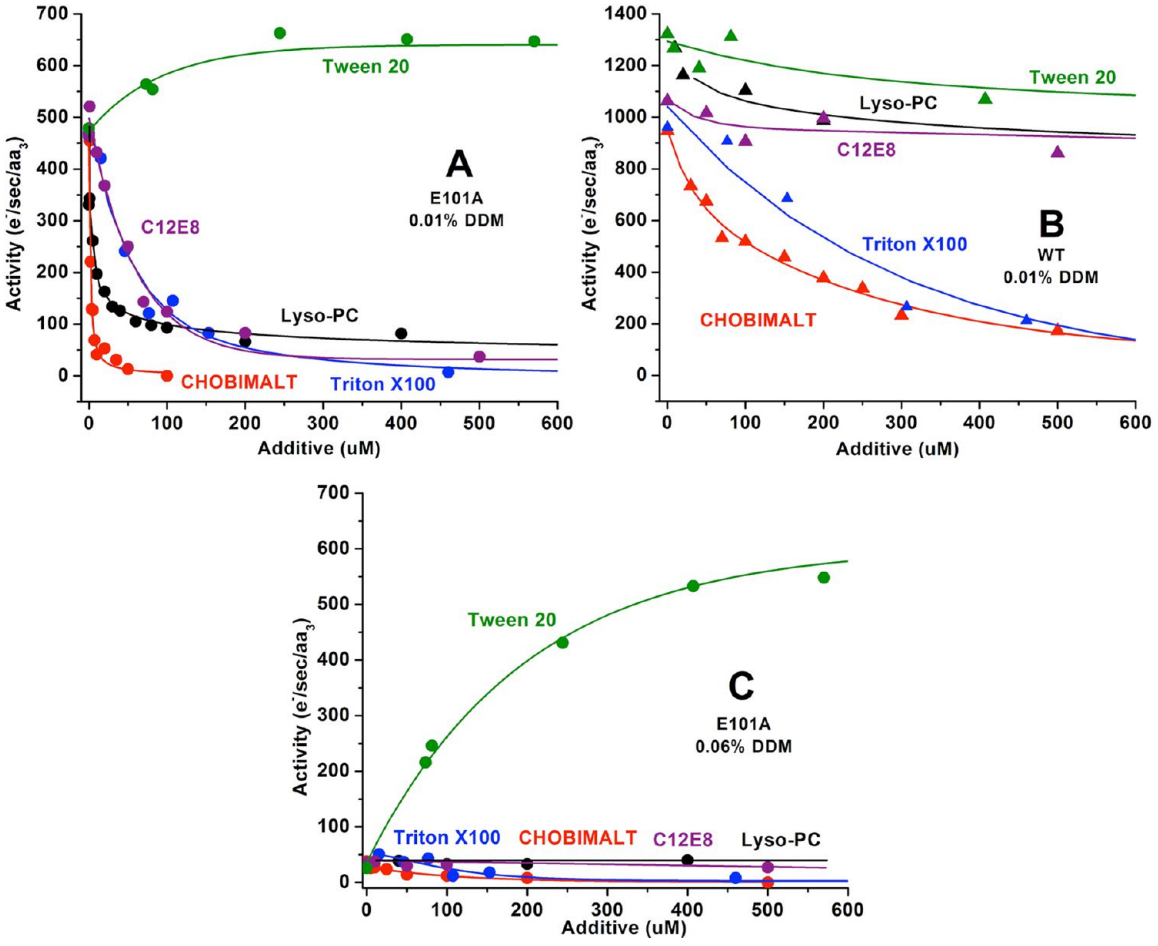

Figure 3. Inhibition of *Rs*C*c*O by lysolipids and detergents. Purified E101A (A, C) and WT (B) *Rs*C*c*O were assayed in 0.01% DDM (A, B) and 0.06% DDM (C) as described in Materials and Methods. Additives: CHOBIMALT (red), C12E8 (purple), lyso-PC (black), Triton X100 (blue), Tween 20 (green).

fatty acids but also steroids, isoprene-derived compounds, branched chains, cyclic groups, and porphyrins.

The Detergent Dodecyl β-D-Maltopyranoside (DDM) Strongly Inhibits E101A Activity. During these studies it was discovered that not only the amphiphilic carboxylate molecules discussed above were capable of modifying the E101A mutant's activity but also the detergent DDM itself. DDM is routinely used to solublize and assay C*c*O since the original finding that it was uniquely effective in dispersing, stabilizing, and activating C*c*O.[44] However, DDM inhibited the E101A mutant even at the relatively low levels (0.06%) normally used for maximally activating the WT *Rs*C*c*O (Figure

dx.doi.org/10.1021/bi3014505 | *Biochemistry* 2013, 52, 1385−1396

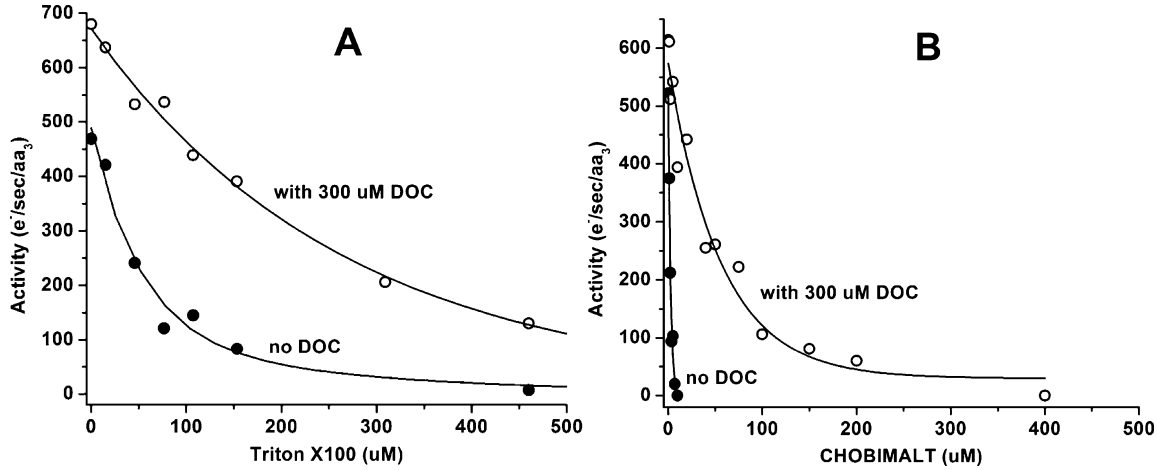

Figure 4. Competition of Triton X100 (A) and CHOBIMALT (B) with deoxycholate (DOC) for activation of E101A *Rs*C*c*O. Purified E101A *Rs*C*c*O was assayed in 0.01% DDM as described in Materials and Methods in the absence (solid circles) and presence (open circles) of 300 μM DOC.

2A). Decyl β-D-maltopyranoside (DM) with the same maltose headgroup but shorter alkyl chain was less inhibitory than DDM, but the α- and β-isomers of DDM had similar effects (data not shown). This indicates that the chain length of the detergent was influential in the effect on E101A activity.

The inhibitory effect of DDM on E101A activity, in contrast to little effect on WT (Figure 2A) or D132A (data not shown), suggests that DDM can bind in the vicinity of the bile acid/steroid site in the E101A mutant and interfere further with the mutant's already inhibited activity (~50% of WT). Therefore DDM appears to compete with other amphipathic ligands, thus complicating the interpretation of the mutant-based assay. The mutant's activity in the presence of any added ligand is then expected to reflect both the ligand's ability to compete with DDM for binding (hence removal of detergent inhibition) and the ligand's own effect once bound (activation or inhibition or both).

Effects of Carboxylate Ligands on E101A Are Altered in Low DDM. To determine the nature of the effect of DDM concentration, ligands were retested in 0.01% DDM, the minimal level required to support enzyme solubility and activity (Figure 2B). Under these low DDM conditions without any additives, the E101A mutant was much more active, showing ~50% of WT activity in 0.01% DDM compared to 5−8% of WT activity in 0.06% DDM (Figure 2A). Indeed, some of the additives that had stimulated the activity of the mutant in 0.06% DDM now inhibited when tested at low DDM (Figure 2B). However, in several cases (e.g., cholesterol hemisuccinate, retinoic acid) stimulation still occurred at low ligand concentrations before inhibition set in, suggesting a complex mode of interaction (see Discussion). It is worth noting that a biphasic ligand effect of stimulation followed by inhibition in the micromolar concentration range was also observed for some ligands even in the higher DDM conditions. Ligand interactions with WT *Rs*C*c*O were less affected by DDM concentration (data not shown).

The soybean phospholipid mixture (asolectin) also stimulated and then inhibited in the 200−1000 μM range, but likely components of this mixture, including cardiolipin and dioleoyl phosphatidylcholine, when tested individually were inhibitory rather than stimulatory (data not shown). The results suggest that the presence of low levels of much more potent effectors, such as long chain fatty acids, account for the asolectin effects.

Other Detergents Inhibit E101A Activity and Wild-Type to a Lesser Extent. The generality of the differential inhibitory effects of DDM on E101A versus WT C*c*O was investigated. The detergent Triton X100 was previously established as an inhibitor of bovC*c*O.[19,45] This detergent strongly inhibited E101A activity ($K_{1/2}$ ~ 50 μM) when assayed at the lowest level of DDM (0.01%) (Figure 3A). Unlike DDM, Triton X100 also inhibited the activity of WT *Rs*C*c*O ($K_{1/2}$ ~ 200 μM) but to a lesser extent (Figure 3B). Inhibition of E101A occurred well below the critical micelle concentration of Triton X100 (230 μM), suggesting that the effect was mediated by Triton X100 monomers rather than by Triton X100 micelles. Neither Triton X100 nor DDM inhibited the D-path mutant D132A (data not shown), supporting the selective interaction of Triton X100 and DDM at the K-path, which is not rate-limiting in the D-path mutant.

The three cholesterol-based detergents digitonin, CHAPS, and CHOBIMALT might be expected to have some affinity for the steroid site. However, CHAPS had been shown to have no effect.[16] CHOBIMALT is potentially a better analogue of cholesterol since its bimaltose headgroup is attached to the single hydroxyl on the A-ring of cholesterol.[46] The activity of E101A was strongly inhibited by CHOBIMALT, even more potently than by DDM or Triton X100, with half-maximal inhibition at ~2 μM in 0.01% DDM (Figure 3A). WT *Rs*C*c*O activity was also inhibited, but 100-fold less with half-maximal inhibition at ~200 μM in 0.01% DDM (Figure 3B). Digitonin, with its very large branched sugar headgroup and modified steroid ring structure, was a less powerful inhibitor, with $K_{1/2}$ in the 200 μM range (data not shown).

Lyso-oleoyl phosphatidycholine (lyso-PC) has detergent characteristics and was reported to stimulate bovC*c*O.[10,11] However, lyso-PC inhibited E101A in 0.01% DDM with half-maximal inhibition at ~17 μM (Figure 3A). It had little effect on WT *Rs*C*c*O in high (data not shown) or low DDM (Figure 3B) and no significant effect on E101A in 0.06% DDM (Figure 3C). Since lyso-PC strongly inhibited E101A only at the lower DDM concentrations, it appeared to compete at the K-path site. Similarly strong inhibition of E101A was observed for the detergent C12E8 in low DDM (Figure 3A), with little effect on

dx.doi.org/10.1021/bi3014505 | *Biochemistry* 2013, 52, 1385−1396

WT (Figure 3B) or at high DDM (Figure 3C). The effects of all these inhibitory detergents at high DDM appear insignificant (Figure 3C) due to the already low activity of the mutant E101A in 0.06% DDM. However, their effects provide a dramatic contrast to Tween 20, which was a remarkable exception to the general rule of strong inhibitory effects on E101A of noncarboxylate detergents. Tween 20 has a 12-carbon alkyl tail like DDM or C12E8, but a bulky branched polyoxyethylene headgroup, unlike the long linear polyoxyethylene ether chains of Triton X100 and C12E8. Instead of inhibiting, it dramatically stimulated the activity of E101A at all DDM concentrations (Figure 3A,C). A model to explain this behavior in terms of adjacent and somewhat overlapping binding sites is discussed below.

Non-Carboxylate Detergents Compete with Deoxycholate for Binding. The differential effects on E101A compared to WT *Rs*C*c*O of all the amphipathic ligands tested, with and without carboxylate groups, suggest that their binding behavior is strongly influenced by the change in chemistry at the mouth of the K-path with the loss of the E101 carboxyl group. This leads to the conclusion that they are exerting their effects by binding in the vicinity of the steroid/bile acid site. So far the position of that site has only been defined crystallographically for DOC in the WT *Rs*C*c*O.[26] While crystallization with the other amphipathic effectors of *Rs*C*c*O and the E101A mutant is currently in progress, some of these ligands were tested for competitive binding at the same site as DOC by comparing their effects on the activity of E101A in the absence or presence of 300 μM DOC. This DOC concentration had a minor activating effect on E101A in 0.01% DDM (Figure 2B) for which a correction was made. The detergents Triton X100 and CHOBIMALT were chosen for competition studies because of their strong inhibitory effects (Figure 3). Triton X100 clearly inhibited E101A less effectively in the presence of DOC ($K_{1/2} \sim 200$ μM) than in its absence ($K_{1/2} \sim 50$ μM) (Figure 4A). Similarly, in the presence of 100 μM Triton X100, DOC was less effective at stimulating E101A (data not shown). CHOBIMALT also inhibited E101A much less effectively in the presence of DOC ($K_{1/2} \sim 50$ μM) than in its absence ($K_{1/2} \sim 5$ μM) (Figure 4B), indicating that both Triton X100 and CHOBIMALT compete with DOC for binding to the steroid site.

Mechanism of Inhibition/Activation of C*c*O by Amphipathic K-Path Ligands. A number of earlier studies have established that the electron transfer equilibrium between heme *a* and heme a_3 in bovC*c*O is inhibited by detergents, including Triton X100,[19] DDM,[19] and cholate.[12] The inhibition has been attributed to blockage of the K-path, which is required for proton uptake to stabilize the reduced state of heme a_3. A similar type of inhibition is observed in the case of K-path mutations.[13,14,17,18] To determine whether alteration of this equilibrium could explain the inhibitory and stimulatory effects of the ligands studied here, a steady-state spectrophotometric method[17] was used to assay the relative levels of reduction of the heme groups in the presence and absence of ligand. The steady-state levels of heme *a* and heme a_3 reduction were measured by comparing the relative absorbances of the α-peak at 607 nm (absorbance contributed ~80% by heme *a*[47]) and the Soret peak at 445 nm (absorbance due to approximately 50% heme *a* and 50% heme a_3[47]) (Figure 5). For the WT *Rs*C*c*O, the change in absorbance of the α and Soret peaks was similar (indicating 29% and 26% reduction, respectively, of the associated hemes), suggesting that the steady-state equilibrium

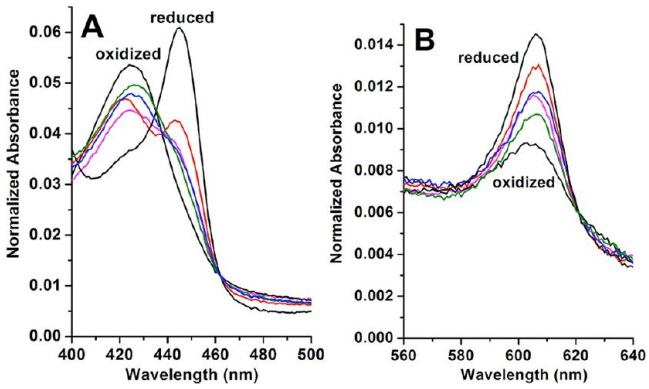

Figure 5. Spectra of purified E101A and WT C*c*O with and without CHOBIMALT. Panel A: Soret region; panel B: α-region. Spectra were normalized to the fully reduced α-peak height at 607−630 nm. Spectra of fully oxidized and fully reduced purified C*c*O are shown in black. Steady-state spectra in 100 mM CHES pH 9.5 with 0.01% DDM were recorded 3 min after adding 1 mM ascorbate and 200 μM TMPD: WT only (green), WT with CHOBIMALT (blue), E101A only (magenta), E101A with CHOBIMALT (red).

favored some electron retention on heme *a* at the high pH necessary to slow the activity of the WT to observe a steady state. For the E101A under the same conditions, the α-peak was more affected (indicating ~51% reduction of associated hemes) than the Soret peak (indicating ~26% reduction), supporting the hypothesis that this mutation alone favored electron retention on heme *a*. Addition of CHOBIMALT to WT also had a selective effect on the α-peak (~43% reduction of associated hemes), implying that the binding of this detergent also impaired ET from heme *a* to a_3. Addition of CHOBIMALT to E101A influenced the equilibrium even further, leading to a strong effect on the α-peak (indicating ~73% reduction of associated hemes) while the Soret peak was affected only to an extent that was accountable by preferential heme *a* reduction (~44%) in the steady state. It should be noted that in the fully reduced and fully oxidized states the addition of CHOBIMALT did not affect the spectra of either WT or E101A. The results are consistent with an inhibitory effect of these E101A ligands on the electron transport equilibrium between the hemes, presumably due to effects on the proton uptake required for heme a_3−Cu_B reduction.

Modeling Alternative Ligand Interactions at the Steroid Site Based on Other Crystal Structures. Given the variety of compounds that appear to interact with relatively high affinity at what was originally observed to be a bile acid/steroid binding site, it is important to note that other structurally characterized proteins show interchangeability of ligands, in particular steroids, porphyrins, and other amphipathic molecules.[30−32] Knowledge of how porphyrin and steroid molecules bind relative to one another in the same site in another protein—mimicking each others' key protein interactions—provides testable information regarding how they might bind relative to one another in the *Rs*C*c*O deoxycholate site. Ferrochelatase has been crystallized with its substrate PPIX and the bile acid cholate,[30,31] showing how a steroid and porphyrin could bind to the same site (Figure 6A). Similarly, human serum albumin has been crystallized with biliverdin, a natively transported heme catabolic product, and fusidic acid, an antibiotic that is structurally similar to bile acids, in the same binding site.[32] To test whether these heme-like ligands could mimic the cholate steroid ring interactions in *Rs*C*c*O in the

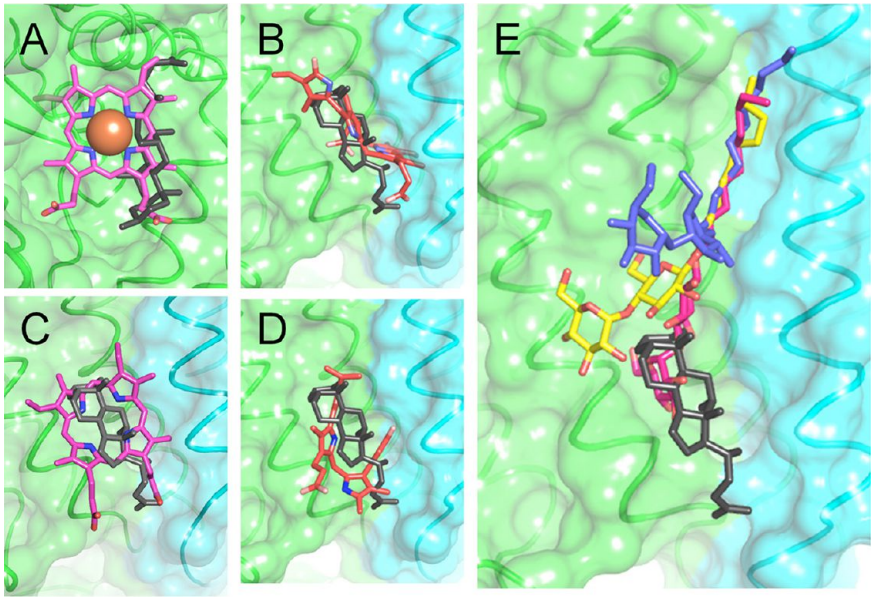

Figure 6. Potential binding orientations of known amphipathic ligands in the *Rs*C*c*O steroid binding site. (A) Heme (magenta sticks) and cholate (black sticks) bound in the same site in two different crystal structures of ferrochelatase (PDB: 2PO7[30] and 2QD2[31]). (B) An energetically favorable orientation of the BR analogue biliverdin (red sticks) in *Rs*C*c*O based on ligand transposition from serum albumin. Energetically favorable *SLIDE* dockings into *Rs*C*c*O of (C) PPIX (magenta sticks), (D) BR (red sticks), and (E) two DDM flexible conformers (yellow and magenta sticks). (B–E) The crystallographically bound deoxycholate (black sticks; PDB: 3DTU[26]) and DDM (blue sticks; PDB 3HB3[4]) are shown as reference molecules.

same orientation they exhibit in serum albumin and ferrochelatase, their PPIX and biliverdin ligands were transposed into the *Rs*C*c*O bile acid/steroid binding site as described in the Materials and Methods. The transposed ferrochelatase heme group interpenetrated the *Rs*C*c*O protein surface, and thus would be sterically disallowed in this binding orientation, while the serum albumin biliverdin was transposed into the *Rs*C*c*O site with no steric hindrance and interacted favorably with *Rs*C*c*O according to *SLIDE* evaluation of $\Delta G_{binding}$ (Figure 6B).

Docking of PPIX and BR into the Steroid Binding Site. Alternative binding interactions for these ligands in the steroid site were identified by *SLIDE* small molecule docking of low-energy PPIX and BR conformers. The top four PPIX dockings (scoring two standard deviations greater than the average docked PPIX score) depicted two possible binding modes in which half the PPIX is located in the steroid site and one propionate group makes protein interactions similar to the DOC carboxyl tail (one mode is shown in Figure 6C). The top eight docked BR conformers (based on *SLIDE* scores at least two standard deviations above the mean) shared a single BR binding mode (Figure 6D). This binding mode, like that of BR in human serum albumin, creates an L-shaped ligand conformation[32] with the BR dipyrinone group located in the same site as the steroid ring. The *SLIDE* docking of PPIX and BR support the likely interaction of these ligands with the steroid binding site and provide testable hypotheses for ligand–protein side-chain interactions.

Modeling Detergent Binding to the *Rs*C*c*O Steroid Binding Region. Predicting possible binding orientations of detergents in the steroid site is currently a significant challenge; however, an alternative interaction mode is suggested by a *Pd*C*c*O crystal structure containing a DDM bound in a unique orientation just above the steroid binding site.[4] In this structure, the maltose headgroup is indicated to be flexible and located in the middle of the membrane region, while the tail is embedded in a hydrophobic groove that is also occupied by an alkyl tail in all oxidase structures (Figure 6E). To test whether the headgroup of this unusual binding orientation of DDM could also interact with the steroid site, low-energy conformations of DM and DDM were docked into the *Pd*C*c*O DDM site by using *SLIDE*. Among the many energetically favorable dockings identified with acyl tails occupying the *Pd*C*c*O DDM site, the maltose headgroup positions varied between being solvent-exposed or protein-associated. In the latter cases, the *Rs*C*c*O steroid binding site was occluded by the headgroup (Figure 6E). This could explain how DDM and certain other detergents compete with bile acid binding while occupying an equally conserved, overlapping region in close proximity. It may also explain the inhibitory effects of the detergents on the E101A mutant, since the detergent headgroup binding in the cholate site could interfere directly with K-path proton uptake.

■ DISCUSSION

This work addresses the effects of various amphipathic and steroid-like molecules that competitively interact at a crystallographically defined bile acid/steroid binding site located at the entrance of the K proton uptake path of bacterial and mammalian C*c*O. It is interesting that none of the more than 50 C*c*O crystal structures in the PDB has any ligand resolved in this site, except the additives cholate or deoxycholate. This suggests that in the native structure this site is not a phospholipid binding site, since detergents such as DM, DDM, or LDAO typically occupy phospholipid sites in the bacterial C*c*O, sites which contain native lipids in the bov*Cc*O.[3]

Comparing the cholate binding site in bov*Cc*O with the DOC site in *Rs*C*c*O indicates that they have important structural similarities beyond their location at the entrance region of the K-path (Supporting Information Table T2). The consensus between cholate and DOC binding includes interactions with the conserved K-path residue E62/E101 (bov/*Rs*) in subunit II, a conserved threonine T66/T105 one

dx.doi.org/10.1021/bi3014505 | *Biochemistry* 2013, 52, 1385–1396

helical turn above this entrance point of the K-path, and positive charges interacting with the carboxyl group consisting of a cadmium ion or a histidine side chain (*Rs*C*c*O) or a pair of arginine residues (bovC*c*O) There is also a lipid or detergent molecule closely associated with the external hydrophobic surface of the bile acid in each case.

Cholate in bovC*c*O contacts subunit VIa of the other monomer in the crystallographic dimer as well as the highly conserved subunit II residue W65, while DOC in *Rs*C*c*O contacts subunit I via conserved residues A319 and P358. In both cases several water molecules are stabilized by the presence of these ligands, participating in their interactions with subunits I and II (Figure 7).

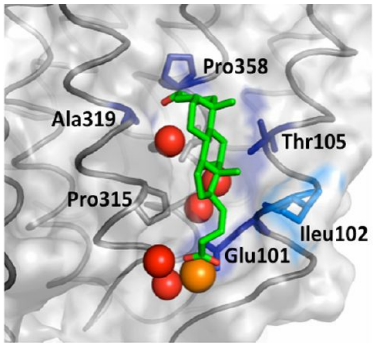

Figure 7. *Rs*C*c*O deoxycholate binding site with conserved residues and bound water molecules (PDB 3DTU[26]). The steroid binding site side chains are colored by degree of conservation in C*c*O sequences as calculated in Buhrow et al.[38] where residues with >75%, 50−75%, or <50% conservation are colored dark blue, medium blue, and gray, respectively. The structure includes a bound deoxycholate (green sticks), K-path water molecules (red spheres), and a cadmium ion (orange sphere).

Mechanisms of Activation/Inhibition of C*c*O by Ligands. There are several potential mechanisms by which amphipathic compounds could activate or inhibit C*c*O by favoring or disfavoring proton uptake in the K-path.

One hypothesis involves the disruption or stabilization by ligand binding of a proton conducting network in the K-path, which involves hydrogen bonded amino acids and water molecules that are likely required for proton transfer. Waters in the lower K-path have been crystallographically resolved in *Pd*C*c*O,[4] *Rs*C*c*O,[48,49] and bovC*c*O (PDB: 2DYR), and a role for E101 in organizing water near the K-path entrance has been invoked for bacterial C*c*Os.[4,6,50] DOC binding results in three well-resolved water molecules binding between the planar ring system of DOC and the lower K-path (Figure 7). The resulting changes in hydrogen bonding at this opening to the K-path may affect the continuity of the pathway or reduce mobility of water molecules involved in conducting protons.

Another possibility (which may coexist with the first) is that the presence of amphipathic ligands in the region associated with the K-path may either promote or restrict conformational change observed to occur in the reduced state,[48,49] which is postulated to be necessary to open the K-path for rapid proton access to the heme a_3 region.[38,48,51] The central region of the K-path (subunit I, helix VIII, residues 355−364) has been shown by H/D exchange to experience altered solvent accessibility upon enzyme reduction.[52] Intrinsic protein flexibility analysis also suggests this region is highly flexible, influencing water molecule positions along the K-path.[38]

Deoxycholate appears to lower the flexibility of C*c*O, based upon lower average *B*-values of WT *Rs*C*c*O crystals with DOC bound.[26] *ProFlex* modeling also suggests that DOC reduces conformational flexibility of the K-path region (Figure 8B,D)

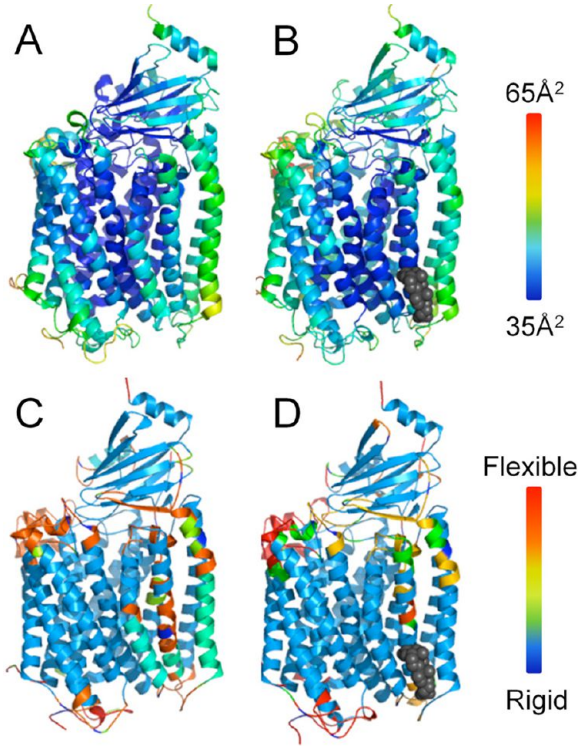

Figure 8. *Rs*C*c*O K-path rigidification upon ligand binding. (A) *Rs*C*c*O (PDB: 2GSM[2]) and (B) deoxycholate-bound *Rs*C*c*O (PDB: 3DTU[26]) are colored by crystallographic *B*-value, where red represents values ≥65 Å², while deep blue represents values ≤35 Å². (C) *Rs*C*c*O and (D) deoxycholate-bound *Rs*C*c*O are colored by internal protein flexibility as determined by the *ProFlex*. Deep blue represents greatest rigidity while red represents greatest flexibility.

relative to the unbound state (Figure 8A,C). In addition, upon reduction of *Rs*C*c*O crystals there is loss of bound DOC, [6] suggesting that ligands like DOC may stabilize the oxidized state and prevent conformational changes required for efficient functioning of the K-path.

Separate but Overlapping Binding Sites for Steroids and Detergents in the K-Path Region. It is a curious observation that the site where cholate (in bovC*c*O) and DOC (in *Rs*C*c*O) is bound is not occupied by any other detergent or lipid molecule in all C*c*O structures so far determined. Nevertheless, our data strongly suggest competition between the bile acids and certain detergents (including DDM) as well as other effector molecules. A possible explanation for this seeming disconnect comes from the recent *Paracoccus* C*c*O structure[4] where a DDM molecule is seen with its maltose headgroup sampling several positions in the membrane region (Figure 2E). Computational analysis (Figure 6E) supports an energetically favorable position with the headgroup overlapping the steroid binding site, which could explain the observed competition with molecules binding in the steroid site. Interestingly, in *Rs*C*c*O and bovC*c*O crystal structures, an alkyl tail is always resolved in the deep groove where the tail of the unusual *Paracoccus* DDM position is located (Figure 9). This region mediates the interaction between subunit I and the

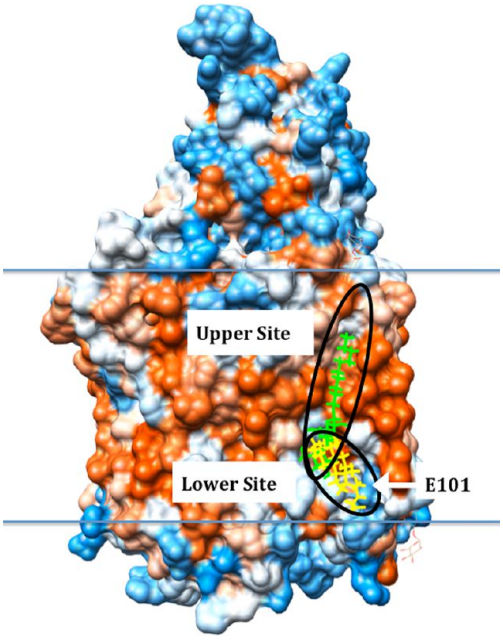

Figure 9. Two-site model for binding of steroids and detergents near the K-path entrance. The lower site is shown with the crystallographic deoxycholate in yellow (from *Rs*C*c*O, PDB: 3DTU[26]). The upper site is shown with the crystallographic DDM in green (from *Pd*C*c*O, PDB: 3HB3[4]) modeled with the flexible headgroup in the most extended position. The surface of the *Rs*C*c*O structure is represented with the hydrophobic regions in dark orange, the hydrophilic charged regions in blue, and neutral regions in pale blue/pale orange/white (Chimera, UCSF). The position of the membrane region is indicated by blue lines.

highly conserved second transmembrane helix of subunit II. In bovC*c*O, the alkyl tail position is occupied by the fatty acid chain of a cardiolipin molecule that connects two monomers at the interface of the dimer.[5]

The working hypothesis arising from these observations is that some of the effectors, particularly long-chain nonionic detergents, may exert their influence by binding at the upper DDM site with their head groups interacting with the lower bile acid/steroid site (Figure 9) blocking the K-path and competing with other ligands. The strength and nature of their competing effects would depend on their headgroup size, chemistry, positioning, and occupancy in the steroid site. The exceptional activating behavior of Tween 20, which has an unusually bulky branch-chain headgroup, can be explained as due to its ability to bind to the upper alkyl chain groove but inability of its headgroup to bind in the membrane region.

The presence of overlapping binding sites raises the question of which molecules fit into which sites. It is predicted from docking and the available data that the bulkier ligands (steroids, porphyrins, branched-chain isoprenes) bind in the lower site and the longer simpler chains (DDM, the Triton X100 polyoxyethylene group, C12E8) bind in the narrower groove provided by the upper site, while some (e.g., long-chain fatty acids, Triton X100) occupy both. However, deciphering the actual binding specificity will require further mutational and crystallographic analysis. An interesting, possibly analogous site has been defined for Complex I[53,54] in which a critical subunit interface region appears to be where quinones, inhibitors, and detergents, including Triton X100 and C12E8 (but not bile acids), bind at overlapping amphipathic sites.

Potential Physiological Implications of the Steroid Site of C*c*O. The physiological significance of this site remains elusive, although the fact that the bile acid/steroid site is conserved from bacteria to mammals and interacts with high affinity with a set of physiologically interesting compounds strengthens the idea that the site is important in regulation of cytochrome *c* oxidase activity.

Studies of purified bovine C*c*O support bile acids[12] as activity regulators. Analyses of mitochondrial function have also implicated glucocorticoids[55] and steroids as strong effectors.[56,57] Whole cell and tissue studies suggest that porphyrins, BR, and bile acids modulate cell fate, specifically at the level of C*c*O activity.[58,59] Together these results suggest that the C*c*O steroid site is sensitive to a variety of physiological ligands with previously uncharacterized molecular effects.

Similarly, isoprene-derived compounds such as thyroid hormone[60,61] have been reported to influence C*c*O activity in mitochondria, findings in accord with the direct effects of cholesteryl hemisuccinate, retinoic acid (Figures 1 and 2) and thyroid hormone (data not shown) on the purified enzyme in our studies. The observation that another isoprene compound, phytanic acid, inhibits C*c*O in rat cerebral cortex homogenates at micromolar levels[62] is consistent with our finding of powerful inhibition of bacterial and mammalian C*c*O.

The original suggestion, based on crystallographic[1] and activity[20,21,63] studies on the mammalian oxidase, was that the cholate sites in bovC*c*O represented adenine nucleotide regulatory sites due to the similar size, shape, and binding characteristics of these ligands.[1] Our current studies do not rule this out, but we did not observe significant effects of adenine nucleotides in the assay systems described here.

Another interesting feature of the ligand binding region we have described in this work is its location at the interface of the crystallographically defined bovC*c*O dimer. The bovC*c*O structure shows a homodimer with two cholate molecules and two cardiolipin molecules resolved at that interface.[5] In fact, one alkyl chain of each cardiolipin molecule is embedded in the groove we have defined as the upper site (Figure 9), the same site observed to bind DDM in *Pd*C*c*O, allowing its headgroup to overlap the steroid site. It is plausible that physiological ligands to this region could control monomer/dimer equilibrium and, in turn, influence formation of the respiratory chain supercomplex with regulatory implications.[64−66]

■ CONCLUSIONS

The current studies report a variety of new ligands that can impact a site that has been defined crystallographically as a bile acid binding site in bacterial and mammalian C*c*O. The results reveal the ability of certain carboxylate and noncarboxylate amphipathic molecules to stimulate or inhibit E101A and WT *Rs*C*c*O by competing for binding in this region. These ligands alter the electron transfer equilibrium between heme *a* and heme a_3, likely by affecting proton uptake in the K-path. Two overlapping sites for steroid and alkyl chain binding at the interface of subunits I and II are proposed to be involved in mediating the observed effects. The results suggest that this conserved site has physiological significance, although further investigation by crystallography, mutagenesis, ligand screening, and modeling will be required to define the native interacting species.

dx.doi.org/10.1021/bi3014505 | *Biochemistry* 2013, 52, 1385−1396

■ ASSOCIATED CONTENT

Supporting Information

Table T1: the structures of the compounds tested on *Rs*C*c*O and discussed in this paper; Table T2: comparison of protein−ligand interactions in the bovC*c*O and *Rs*C*c*O bile acid/steroid binding sites. This material is available free of charge via the Internet at http://pubs.acs.org.

■ AUTHOR INFORMATION

Corresponding Author

*Phone (517)-355-0199; e-mail fergus20@msu.edu.

Author Contributions

†These authors contributed equally to this work.

Funding

This work was supported by NIH GM26916 (SF-M).

Notes

The authors declare no competing financial interest.

■ ACKNOWLEDGMENTS

The authors thank OpenEye Scientific Software (Santa Fe, NM[35]) for academic licensing of their software.

■ ABBREVIATIONS

BovC*c*O, C*c*O from *Bos taurus* (bovine heart); BR, bilirubin; C*c*O, cytochrome *c* oxidase; chenoDOC, chenodeoxycholate; CHS, cholesteryl hemisuccinate; DDM, dodecyl maltoside (lauryl maltoside); DM, decyl maltoside; DOC, deoxycholate; ET, electron transfer; glycochenoDOC, glycochenodeoxycholate; GUDCA, glycoursodeoxycholate; lyso-PC, 18:1 lysophosphatidylcholine (lyso-oleoyl phosphatidylcholine); PDB, Protein Data Bank; *Pd*C*c*O, C*c*O from *Paracoccus denitrificans*; PPIX, protoporphyrin IX; *Rs*, *Rhodobacter sphaeroides*; *Rs*C*c*O, C*c*O from *Rhodobacter sphaeroides*; TN, turnover number (electrons per second per C*c*O molecule); ursoDOC, ursodeoxycholate; WT, wild-type.

■ REFERENCES

(1) Tsukihara, T., Aoyama, H., Yamashita, E., Tomizaki, T., Yamaguchi, H., ShinzawaItoh, K., Nakashima, R., Yaono, R., and Yoshikawa, S. (1996) The whole structure of the 13-subunit oxidized cytochrome *c* oxidase at 2.8 angstrom. *Science 272*, 1136−1144.

(2) Qin, L., Hiser, C., Mulichak, A., Garavito, R. M., and Ferguson-Miller, S. (2006) Identification of conserved lipid/detergent-binding sites in a high-resolution structure of the membrane protein cytochrome *c* oxidase. *Proc. Natl. Acad. Sci. U.S.A. 103*, 16117−16122.

(3) Qin, L., Sharpe, M. A., Garavito, R. M., and Ferguson-Miller, S. (2007) Conserved lipid-binding sites in membrane proteins: a focus on cytochrome *c* oxidase. *Curr. Opin. Struct. Biol. 17*, 444−450.

(4) Koepke, J., Olkhova, E., Angerer, H., Muller, H., Peng, G., and Michel, H. (2009) High resolution crystal structure of *Paracoccus denitrificans* cytochrome *c* oxidase: new insights into the active site and the proton transfer pathways. *Biochim. Biophys. Acta 1787*, 635−645.

(5) Shinzawa-Itoh, K., Aoyama, H., Muramoto, K., Terada, H., Kurauchi, T., Tadehara, Y., Yamasaki, A., Sugimura, T., Kurono, S., Tsujimoto, K., Mizushima, T., Yamashita, E., Tsukihara, T., and Yoshikawa, S. (2007) Structures and physiological roles of 13 integral lipids of bovine heart cytochrome *c* oxidase. *EMBO J. 26*, 1713−1725.

(6) Ferguson-Miller, S., Hiser, C., and Liu, J. (2012) Gating and regulation of the cytochrome *c* oxidase proton pump. *Biochim. Biophys. Acta 1817*, 489−494.

(7) Brierley, G. P., and Merola, A. J. (1962) Studies of Electron-Transfer System. 48. Phospholipid Requirements in Cytochrome Oxidase. *Biochim. Biophys. Acta 64*, 205−217.

(8) Vanneste, W. H., Ysebaert., M., and Mason, H. S. (1974) Decline of Molecular Activity of Cytochrome-Oxidase during Purification. *J. Biol. Chem. 249*, 7390−7401.

(9) Yu, C. A., Yu, L., and King, T. E. (1975) Studies on Cytochrome-Oxidase - Interactions of Cytochrome-Oxidase Protein with Phospholipids and Cytochrome-C. *J. Biol. Chem. 250*, 1383−1392.

(10) Vik, S. B., and Capaldi, R. A. (1977) Lipid Requirements for Cytochrome-C Oxidase Activity. *Biochemistry 16*, 5755−5759.

(11) Vik, S. B., and Capaldi, R. A. (1980) Conditions for Optimal Electron-Transfer Activity of Cytochrome-C Oxidase Isolated from Beef-Heart Mitochondria. *Biochem. Biophys. Res. Commun. 94*, 348−354.

(12) Van Buuren, K. J. H., and Van Gelder, B. F. (1974) Biophysical Studies on Cytochrome-*c* Oxidase. 13. Effect of Cholate on Enxymic Activity. *Biochim. Biophys. Acta 333*, 209−217.

(13) Branden, M., Tomson, F., Gennis, R. B., and Brzezinski, P. (2002) The entry point of the K-proton-transfer pathway in cytochrome *c* oxidase. *Biochemistry 41*, 10794−10798.

(14) Tomson, F. L., Morgan, J. E., Gu, G. P., Barquera, B., Vygodina, T. V., and Gennis, R. B. (2003) Substitutions for glutamate 101 in subunit II of cytochrome *c* oxidase from *Rhodobacter sphaeroides* result in blocking the proton-conducting K-channel. *Biochemistry 42*, 1711−1717.

(15) Ma, J. X., Tsatsos, P. H., Zaslavsky, D., Barquera, B., Thomas, J. W., Katsonouri, A., Puustinen, A., Wikstrom, M., Brzezinski, P., Alben, J. O., and Gennis, R. B. (1999) Glutamate-89 in subunit II of cytochrome bo_3 from *Escherichia coli* is required for the function of the heme-copper oxidase. *Biochemistry 38*, 15150−15156.

(16) Qin, L., Mills, D. A., Hiser, C., Murphree, A., Garavito, R. M., Ferguson-Miller, S., and Hosler, J. (2007) Crystallographic location and mutational analysis of Zn and Cd inhibitory sites and role of lipidic carboxylates in rescuing proton path mutants in cytochrome *c* oxidase. *Biochemistry 46*, 6239−6248.

(17) Konstantinov, A. A., Siletsky, S., Mitchell, D., Kaulen, A., and Gennis, R. B. (1997) The roles of the two proton input channels in cytochrome *c* oxidase from *Rhodobacter sphaeroides* probed by the effects of site-directed mutations on time-resolved electrogenic intraprotein proton transfer. *Proc. Natl. Acad. Sci. U.S.A. 94*, 9085−9090.

(18) Vygodina, T. V., Pecoraro, C., Mitchell, D., Gennis, R., and Konstantinov, A. A. (1998) Mechanism of inhibition of electron transfer by amino acid replacement K362M in a proton channel of *Rhodobacter sphaeroides* cytochrome *c* oxidase. *Biochemistry 37*, 3053−3061.

(19) Antalik, M., Jancura, D., Palmer, G., and Fabian, M. (2005) A role for the protein in internal electron transfer to the catalytic center of cytochrome *c* oxidase. *Biochemistry 44*, 14881−14889.

(20) Frank, V., and Kadenbach, B. (1996) Regulation of the H +/e(−) stoichiometry of cytochrome *c* oxidase from bovine heart by intramitochondrial ATP/ADP ratios. *FEBS Lett. 382*, 121−124.

(21) Arnold, S., and Kadenbach, B. (1997) Cell respiration is controlled by ATP, an allosteric inhibitor of cytochrome-*c* oxidase. *Eur. J. Biochem. 249*, 350−354.

(22) Napiwotzki, J., ShinzawaItoh, K., Yoshikawa, S., and Kadenbach, B. (1997) ATP and ADP bind to cytochrome *c* oxidase and regulate its activity. *J. Biol. Chem. 378*, 1013−1021.

(23) Ludwig, B., Bender, E., Arnold, S., Huttemann, M., Lee, I., and Kadenbach, B. (2001) Cytochrome *c* oxidase and the regulation of oxidative phosphorylation. *ChemBioChem 2*, 392−403.

(24) Kadenbach, B. (2003) Intrinsic and extrinsic uncoupling of oxidative phosphorylation. *Biochim. Biophys. Acta, Bioenerg. 1604*, 77−94.

(25) Shoji, K., Giuffre, A., D'Itri, E., Hagiwara, K., Yamanaka, T., Brunori, M., and Sarti, P. (2000) The ratio between the fast and slow forms of bovine cytochrome c oxidase is changed by cholate or nucleotides bound to the cholate-binding site close to the cytochrome a_3/Cu_B binuclear centre. *Cell. Mol. Life Sci. 57*, 1482−1487.

(26) Qin, L., Mills, D. A., Buhrow, L., Hiser, C., and Ferguson-Miller, S. (2008) A conserved steroid binding site in cytochrome *c* oxidase. *Biochemistry 47*, 9931−9933.
(27) Hiser, C., Mills, D. A., Schall, M., and Ferguson-Miller, S. (2001) C-terminal truncation and histidine-tagging of cytochrome *c* oxidase subunit II reveals the native processing site, shows involvement of the C-terminus in cytochrome *c* binding, and improves the assay for proton pumping. *Biochemistry 40*, 1606−1615.
(28) Suarez, M. D., Revzin, A., Narlock, R., Kempner, E. S., Thompson, D. A., and Ferguson-Miller, S. (1984) The Functional and Physical Form of Mammalian Cytochrome *c* Oxidase Determined by Gel-Filtration, Radiation Inactivation, and Sedimentation Equilibrium-Analysis. *J. Biol. Chem. 259*, 3791−3799.
(29) Hosler, J. P., Fetter, J., Tecklenburg, M. M. J., Espe, M., Lerma, C., and Ferguson-Miller, S. (1992) Cytochrome aa_3 of *Rhodobacter sphaeroides* as a Model for Mitochondrial Cytochrome *c* Oxidase - Purification, Kinetics, Proton Pumping, and Spectral-Analysis. *J. Biol. Chem. 267*, 24264−24272.
(30) Dailey, H. A., Wu, C. K., Horanyi, P., Medlock, A. E., Najahi-Missaoui, W., Burden, A. E., Dailey, T. A., and Rose, J. (2007) Altered orientation of active site residues in variants of human ferrochelatase. Evidence for a hydrogen bond network involved in catalysis. *Biochemistry 46*, 7973−7979.
(31) Medlock, A. E., Dailey, T. A., Ross, T. A., Dailey, H. A., and Lanzilotta, W. N. (2007) A pi-helix switch selective for porphyrin deprotonation and product release in human ferrochelatase. *J. Mol. Biol. 373*, 1006−1016.
(32) Zunszain, P. A., Ghuman, J., McDonagh, A. F., and Curry, S. (2008) Crystallographic analysis of human serum albumin complexed with 4Z,15E-bilirubin-IX alpha. *J. Mol. Biol. 381*, 394−406.
(33) Schnecke, V., Swanson, C. A., Getzoff, E. D., Tainer, J. A., and Kuhn, L. A. (1998) Screening a peptidyl database for potential ligands to proteins with side-chain flexibility. *Proteins: Struct. Funct. Genet. 33*, 74−87.
(34) Zavodszky, M. I., Sanschagrin, P. C., Korde, R. S., and Kuhn, L. A. (2002) Distilling the essential features of a protein surface for improving protein-ligand docking, scoring, and virtual screening. *J. Comput.-Aided Mol. Des. 16*, 883−902.
(35) Hawkins, P. C. D., Skillman, A. G., Warren, G. L., Ellingson, B. A., and Stahl, M. T. (2010) Conformer Generation with OMEGA: Algorithm and Validation Using High Quality Structures from the Protein Databank and Cambridge Structural Database. *J. Chem. Inf. Model. 50*, 572−584.
(36) Landau, M., Mayrose, I., Rosenberg, Y., Glaser, F., Martz, E., Pupko, T., and Ben-Tal, N. (2005) ConSurf 2005: the projection of evolutionary conservation scores of residues on protein structures. *Nucleic Acids Res. 33*, W299−W302.
(37) Jacobs, D. J., Rader, A. J., Kuhn, L. A., and Thorpe, M. F. (2001) Protein flexibility predictions using graph theory. *Proteins: Struct. Funct. Genet. 44*, 150−165.
(38) Buhrow, L., Ferguson-Miller, S., and Kuhn, L. A. (2012) From Static Structure to Living Protein: Computational Analysis of Cytochrome *c* Oxidase Main-chain Flexibility. *Biophys. J. 102*, 2158−2166.
(39) Fetter, J., Sharpe, M., Qian, J., Mills, D., Ferguson-Miller, S., and Nicholls, P. (1996) Fatty acids stimulate activity and restore respiratory control in a proton channel mutant of cytochrome *c* oxidase. *FEBS Lett. 393*, 155−160.
(40) Verhoeven, N. M., Wanders, R. J., Poll-The, B. T., Saudubray, J. M., and Jakobs, C. (1998) The metabolism of phytanic acid and pristanic acid in man: a review. *J. Inherited Metab. Dis. 21*, 697−728.
(41) Kruska, N., and Reiser, G. (2011) Phytanic acid and pristanic acid, branched-chain fatty acids associated with Refsum disease and other inherited peroxisomal disorders, mediate intracellular Ca^{2+} signaling through activation of free fatty acid receptor GPR40. *Neurobiol. Dis. 43*, 465−472.
(42) Hellgren, L. I. (2010) Phytanic acid–an overlooked bioactive fatty acid in dairy fat? *Ann. N.Y. Acad. Sci. 1190*, 42−49.
(43) Amengual, J., Ribot, J., Bonet, M. L., and Palou, A. (2008) Retinoic acid treatment increases lipid oxidation capacity in skeletal muscle of mice. *Obesity 16*, 585−591.
(44) Rosevear, P., VanAken, T., Baxter, J., and Ferguson-Miller, S. (1980) Alkyl glycoside detergents: a simpler synthesis and their effects on kinetic and physical properties of cytochrome *c* oxidase. *Biochemistry 19*, 4108−4115.
(45) Mahapatro, S. N., and Robinson, N. C. (1990) Effect of Changing the Detergent Bound to Bovine Cytochrome-*c* Oxidase Upon Its Individual Electron-Transfer Steps. *Biochemistry 29*, 764−770.
(46) Howell, S. C., Mittal, R., Huang, L. J., Travis, B., Breyer, R. M., and Sanders, C. R. (2010) CHOBIMALT: A Cholesterol-Based Detergent. *Biochemistry 49*, 9572−9583.
(47) Vanneste, W. H. (1966) Stoichiometry and Absorption Spectra of Components *a* and a_3 in Cytochrome *c* Oxidase. *Biochemistry 5*, 838−848.
(48) Qin, L., Liu, J., Mills, D. A., Proshlyakov, D. A., Hiser, C., and Ferguson-Miller, S. (2009) Redox-Dependent Conformational Changes in Cytochrome *c* Oxidase Suggest a Gating Mechanism for Proton Uptake. *Biochemistry 48*, 5121−5130.
(49) Liu, J. A., Qin, L., and Ferguson-Miller, S. (2011) Crystallographic and online spectral evidence for role of conformational change and conserved water in cytochrome oxidase proton pump. *Proc. Natl. Acad. Sci. U.S.A. 108*, 1284−1289.
(50) Sharpe, M. A., Qin, L., and Ferguson-Miller, S. (2005) Proton Entry, Exit and Pathways in Cytochrome Oxidase: Insight from Conserved Water, in *Biophysical and Structural Aspects of Bioenergetics* (Wikstrom, M., Ed.) pp 26−54, The Royal Society of Chemistry, Cambridge, UK.
(51) Sharpe, M. A., and Ferguson-Miller, S. (2008) A chemically explicit model for the mechanism of proton pumping in heme-copper oxidases. *J. Bioenerg. Biomembr. 40*, 541−549.
(52) Busenlehner, L. S., Salomonsson, L., Brzezinski, P., and Armstrong, R. N. (2006) Mapping protein dynamics in catalytic intermediates of the redox-driven proton pump cytochrome *c* oxidase. *Proc. Natl. Acad. Sci. U.S.A. 103*, 15398−15403.
(53) Fendel, U., Tocilescu, M. A., Kerscher, S., and Brandt, U. (2008) Exploring the inhibitor binding pocket of respiratory complex I. *Biochim. Biophys. Acta, Bioenerg. 1777*, 660−665.
(54) Okun, J. G., Lummen, P., and Brandt, U. (1999) Three classes of inhibitors share a common binding domain in mitochondrial complex I (NADH:ubiquinone oxidoreductase). *J. Biol. Chem. 274*, 2625−2630.
(55) Simon, N., Jolliet, P., Morin, C., Zini, R., Urien, S., and Tillement, J. P. (1998) Glucocorticoids decrease cytochrome *c* oxidase activity of isolated rat kidney mitochondria. *FEBS Lett. 435*, 25−28.
(56) Molano, F., Saborido, A., Delgado, J., Moran, M., and Megias, A. (1999) Rat liver lysosomal and mitochondrial activities are modified by anabolic-androgenic steroids. *Med. Sci. Sports Exercise 31*, 243−250.
(57) Starkov, A. A., Simonyan, R. A., Dedukhova, V. I., Mansurova, S. E., Palamarchuk, L. A., and Skulachev, V. P. (1997) Regulation of the energy coupling in mitochondria by some steroid and thyroid hormones. *Biochim. Biophys. Acta, Bioenerg. 1318*, 173−183.
(58) Vaz, A. R., Delgado-Esteban, M., Brito, M. A., Bolanos, J. P., Brites, D., and Almeida, A. (2010) Bilirubin selectively inhibits cytochrome c oxidase activity and induces apoptosis in immature cortical neurons: assessment of the protective effects of glycoursodeoxycholic acid. *J. Neurochem. 112*, 56−65.
(59) Malik, S. G., Irwanto, K. A., Ostrow, J. D., and Tiribelli, C. (2010) Effect of bilirubin on cytochrome *c* oxidase activity of mitochondria from mouse brain and liver. *BMC Res. Notes 3*, 162−167.
(60) Goglia, F. (2005) Biological effects of 3,5-diiodothyronine (T-2). *Biochemistry (Moscow) 70*, 164−172.
(61) Arnold, S., Goglia, F., and Kadenbach, B. (1998) 3,5-Diiodothyronine binds to subunit Va of cytochrome-*c* oxidase and abolishes the allosteric inhibition of respiration by ATP. *Eur. J. Biochem. 252*, 325−330.

(62) Busanello, E. N. B., Viegas, C. M., Moura, A. P., Tonin, A. M., Grings, M., Vargas, C. R., and Wajner, M. (2010) In vitro evidence that phytanic acid compromises Na^+, K^+-ATPase activity and the electron flow through the respiratory chain in brain cortex from young rats. *Brain Res. 1352*, 231−238.
(63) Kadenbach, B., Napiwotzki, J., Frank, V., Arnold, S., Exner, S., and Huttemann, M. (1998) Regulation of energy transduction and electron transfer in cytochrome *c* oxidase by adenine nucleotides. *J. Bioenerg. Biomembr. 30*, 25−33.
(64) Dudkina, N. V., Kouril, R., Peters, K., Braun, H. P., and Boekema, E. J. (2010) Structure and function of mitochondrial supercomplexes. *Biochim. Biophys. Acta 1797*, 664−670.
(65) Althoff, T., Mills, D. J., Popot, J. L., and Kuhlbrandt, W. (2011) Arrangement of electron transport chain components in bovine mitochondrial supercomplex $I_1III_2IV_1$. *EMBO J. 30*, 4652−4664.
(66) Bottinger, L., Horvath, S. E., Kleinschroth, T., Hunte, C., Daum, G., Pfanner, N., and Becker, T. (2012) Phosphatidylethanolamine and Cardiolipin Differentially Affect the Stability of Mitochondrial Respiratory Chain Supercomplexes. *J. Mol. Biol. 423*, 677−686.